JOURNAL OF PROPULSION AND POWER
Vol. 22, No. 2, March–April 2006

Modeling of Plasma Virtual Shape Control of Ram/Scramjet Inlet and Isolator

M. N. Shneider* and S. O. Macheret†
Princeton University, Princeton, New Jersey 08544

The paper explores a reverse energy bypass concept of ram/scramjet propulsion control by energy addition and extraction in the propulsion flowpath. Instead of variable geometry, the concept relies on virtual shapes created by plasma/magnetohydrodynamic (MHD) devices or by other methods (including plasma-controlled external combustion). An inherent advantage of the proposed plasma/MHD control system is its flexibility, fast response, and the absence of moving parts. The fixed geometry is optimized for Mach 7 flight. At Mach numbers below the design value, inlet performance can be controlled by energy addition, with the power supplied by an MHD generator placed downstream of the combustor. This concept is called the reverse energy bypass. In one scenario, the inlet flow spillage can be reduced by a virtual cowl—a heated region placed upstream of and slightly below the cowl. With an optimally located virtual cowl, calculations with conservative assumption regarding power transmission losses show that the reverse bypass can increase thrust by about 10% at Mach 6. In another scenario, distributed heating of the flow upstream of the inlet throat in the ramjet regime (Mach 4–6), with the heating rate of about 6.3–8.5% of the total enthalpy flux, can bring the throat Mach number close to one, thus making the isolator duct virtually unnecessary. Although the reverse bypass system with inlet heating would reduce thrust by about 16% at Mach 5, the performance penalty at the vehicle acceleration stage can be offset by the increased efficiency during cruise because of the absence of weight and cooling burdens, which would normally arise from using a long isolator duct.

I. Introduction

THE development of viable hypersonic airbreathing combined-cycle cruise and space launch vehicles faces a number of technical challenges.[1] Some of these challenges stem from the need to operate in a wide range of Mach numbers. For example, as the vehicle passes through approximately Mach 3.5–4, the engine needs to change from turbine operation to ramjet operation. This process will likely involve a change in the flowpath and requires a guaranteed starting mechanism for the ramjet engine to assure that the transition occurs smoothly. Normally that starting mechanism involves reducing the contraction ratio by opening up the inlet, isolator, and engine flowpath cross-sectional area or rotating the cowl leading edge to reduce the air capture ratio.[2] The contraction ratio is then increased by reducing the area or rotating the cowl leading edge to improve the compression and produce acceptable engine performance. The changes in contraction ratio would conventionally be brought out by a complex, heavy, and slow-reacting electrohydraulic system.

The ramjet engine needs to operate with subsonic or transonic air entering the combustor. Typically, this is achieved using a long isolator stage, which acts as a supersonic diffuser to slow the inlet flow to subsonic Mach numbers.[2] Under high-speed operation, there are no strong shocks in the isolator, just a weak oblique shock system downstream of the throat. This results in small inlet losses and a clean profile at entry to the combustor, but it requires significant length to keep the adverse pressure gradients small and avoid separation. Furthermore, it is necessary to ensure that the terminal shock does not move upstream of the throat because the shock position is unstable under these conditions, and the engine will unstart. Normally, strong suction is used to control the shock position and avoid unstart, adding to the overall weight and complexity of the engine.

The ramjet is only used to accelerate the vehicle up to about Mach 5 or 6, at which point the scramjet takes over. Cruise conditions are hypersonic: there is no "design" condition for the ramjet because it is only a transitional stage. Consequently, 1) some level of performance loss can be tolerated during the transient ramjet operation; 2) a long isolator stage adds considerable weight to the engine; and 3) the isolator interior contribute a major part to the cooling load, particularly at high Mach number when the isolator is still in the flowpath, but not needed. In the recent paper,[3] we proposed the use of heat addition upstream of the inlet throat to reduce the Mach number and thus substantially shorten or even eliminate the isolator. Although a substantial amount of power would be needed for this heat addition, and stagnation pressure would be reduced, the thrust penalty in the acceleration stage can be offset by the increased performance during the hypersonic cruise stemming from the shortening or elimination of the isolator.

Another group of challenges is associated with the need to optimize the inlet geometry. The optimum geometry corresponds to the well-known shock-on-lip (SOL) condition: the compression ramp shocks converge on the cowl lip, and the reflected shock impinges on the upper wall of the inlet.[1] Because shock angles are determined by the flight Mach number, the SOL condition cannot be met at Mach numbers higher or lower than the design Mach number.[1] At Mach numbers higher than the design value, the shocks move inside the inlet, causing multiple reflected shocks, loss of stagnation pressure, possible boundary-layer separation, and engine unstart. At Mach numbers lower than the design value, a portion of the air compressed by the shock misses the inlet (spillage), and the air mass capture decreases.

At off-design Mach numbers, energy addition to or extraction from the flow, using plasmas and various magnetohydrodynamic (MHD) devices, can be considered as an alternative to a variable geometry inlet. An important advantage of plasma-based methods of inlet and isolator control is their flexibility, controllability, and fast response.

Presented as Paper 2004-2662 at the AIAA 35th Plasmadynamics and Lasers Conference, Portland, OR, 28 June–1 July 2004; received 3 April 2005; revision received 17 July 2005; accepted for publication 12 August 2005.

*Research Scientist, Department of Mechanical and Aerospace Engineering, D-414 Engineering Quadrangle; shneyder@princeton.edu. Senior Member AIAA.

†Senior Research Scientist, Department of Mechanical and Aerospace Engineering, D-418 Engineering Quadrangle; macheret@princeton.edu. Associate Fellow AIAA.

At Mach numbers higher than the design value, it can be possible to move the shocks from inside the inlet back to the cowl lip by an MHD generator device placed at one of the compression ramps. This method, while providing some flexibility of flow control, would not require any net power to run the MHD device because the generator mode would be used, and the power requirements for air ionization can be minimized with electron beams as ionizers.[4–13] Principal disadvantages of the method include stagnation pressure losses caused by the inevitable Joule heating and also weight of the magnet and other hardware.

In our papers,[4–6,8–13] we demonstrated that this approach to MHD inlet control can yield an acceptable inlet performance, while operating in the mode of net power extraction. We showed that the MHD region should be quite short (typically 25–30 cm along the flow) and be located as far upstream as possible.[4,6]

To increase air mass capture and reduce spillage in scramjet inlets at Mach numbers below the design value, we have suggested the use of energy addition to the flow off the vehicle.[14] The heated region would create a virtual cowl that would deflect the flow streamlines into the inlet.[14] Various mechanisms of energy addition can be used. For example, the heated region can be generated by supplying microwave or RF energy to a volume pre-ionized by a focused laser or electron beam. Other possible means include plasma or hot-air jets, and external combustion. An important advantage of the new method is that the air entering the inlet would have experienced little or no heating.[14] Thus, irreversibilities and stagnation pressure losses associated with heating can be minimized. Optimization studies showed that the best location for the energy addition region is near the intersection of the nose shock of the vehicle with the continuation of the cowl line and slightly below that line.[14]

The primary goal of the present paper is to theoretically explore the possibility of minimizing the need for the traditional isolator stage, as well as increasing the inlet mass capture at Mach numbers below the design value, using active control based on virtual shapes created by energy addition upstream of the inlet throat.[3,14] The virtual shapes can be created by, for example, microwave plasma heating, MHD forces, electron beams, and localized plasma-assisted surface combustion. The power necessary to operate plasmas can come either from the turbine at mode transition, from an auxiliary power unit, or from an MHD generator either placed downstream of the combustor or collocated with it.

In the latter case, MHD power extraction downstream of the combustor and the use of power to control the inlet constitute an energy bypass system, which will be called the reverse energy bypass in this paper. In our recent work,[3] a simple one-dimensional model of MHD power generation downstream of scramjet combustors was developed, and power generation performance is predicted for a variety of generic ydrogen-fueled engine regimes. In this paper, we use the earlier developed model of an MHD generator downstream of the combustor together with the results of virtual cowl and inlet heating modeling to calculate the changes in thrust brought about by the reverse energy bypass system.

II. Virtual Shapes for Inlet/Isolator Control

In the present paper, we use a generic fixed two-ramp forebody geometry designed for shock-on-lip condition at cruise Mach 7 (Ref. 3). At Mach numbers greater than seven, we had proposed using an on-ramp MHD flow/shock control in conjunction with ionization of the cold flow by electron beams[4–6,8–13] and had demonstrated the possibility of restoring the shock-on-lip condition at Mach 8, while powering the ionizing electron beams with the MHD-generated power, at acceptable levels of kinetic energy efficiency of the inlet.

To improve the performance at Mach numbers lower than the design value, the following applications of virtual shapes created by energy addition are explored in the paper:

1) To reduce the spillage drag at Mach numbers lower than the fixed geometry inlet design Mach-number value, a virtual cowl concept,[14] that is, heating the flow upstream of the cowl lip, can be used to divert additional air into the inlet. In this work, we compute mass capture increase by using a virtual cowl at Mach numbers of 5 and 6.

2) To minimize the isolator length, we explore the use of heat addition upstream of the inlet throat.[3] The heating should reduce the Mach number at the throat to that slightly above Mach 1.

3) Based on the earlier developed model of an MHD generator downstream of the combustor,[3] we investigate whether at moderate magnetic field strengths (on the order of 1 T) and at moderate fractions of alkali seed, a megawatt-scale power sufficient to enable the virtual shape inlet control can be generated.

The design Mach 7 geometry and the static temperature and Mach-number contours, as well as the streamlines, are shown in Fig. 1. The freestream dynamics pressure was $q = 1000$ psf (47.88 kPa). The compression ratio here is 62.4, the kinetic energy efficiency is 0.97, and the average Mach number at the throat is 2.77. The freestream conditions in all the cases studied in this paper are listed in Table 1.

The model and governing equations are those of Ref. 14. The inlet flow upstream of the throat is two dimensional in (x, z) plane, where x is the freestream flow direction and z is directed from the vehicle nose upward. Cases both without and with heat addition are computed with the set of Euler equations together with perfect gas equation of state. Volumetric heat-addition term with a prescribed profile was added to the enthalpy equation. Thus, vibrational excitation and relaxation were ignored. Because the entire flow region is supersonic, a steady-state solution using x as a marching coordinate can be found. The inlet performance is characterized by the mass capture coefficient k_m, the compression ratio k_p, the adiabatic

Table 1 Freestream conditions in computed cases[a]

Mach number	Altitude h, km	Static pressure p_0, Pa	Static temperature T_0, K
4	21.0	4729	217.58
5	24.538	2735	221.09
6	26.93	1900	223.47
7	28.974	1395.92	225.49

[a]Freestream dynamic pressure is $q = 1000$ psf (47.88 kPa) in all cases except Mach 4; the dynamic pressure at Mach 4 is $q = 1041$ psf (49.84 kPa).

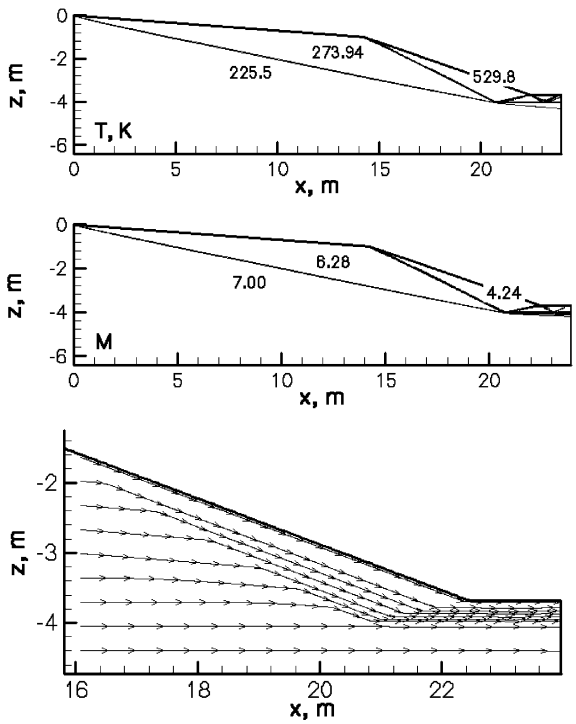

Fig. 1 Contour lines of static temperature and Mach number and flow streamlines in the Mach 7, $q = 1000$ psf (47.88 kPa) design case.

kinetic energy efficiency $\eta_{\mathrm{KE.ad}}$, the average Mach number at the throat $\langle M \rangle$, the enthalpy capture ratio k_H, and the enthalpy flux through the throat $\dot{H}$ per unit length in the spanwise direction. Note that the total (stagnation) pressure at the inlet throat is uniquely related to the kinetic energy efficiency; thus, the stagnation pressure is not listed in the results as it would be a redundant parameter in our calculations.

In most cases, the flow at the inlet throat is quite nonuniform and not parallel to the walls. Therefore, a proper procedure of averaging flow parameters at the throat has to be employed. In this work, as in Refs. 5 and 14, we used the so-called stream-thrust averaging commonly accepted in inlet design.[2] This procedure, described in Ref. 2, effectively takes into account losses of total pressure (entropy increase) that would occur downstream of the throat, in the isolator, when the flow is allowed to settle and to become parallel to the walls.

All computations in this work were performed with $12{,}500 \times 240$ grid. Variation of the number of grid points in each of the two dimensions by a factor of 2 resulted in negligible (less than 0.5%) variation of the results.

A. Air Capture Increase with Virtual Cowl

To reduce the spillage drag at Mach numbers lower than the fixed geometry inlet design Mach-number value, a virtual cowl concept,[14] that is, heating the flow upstream of the cowl lip, can be used to divert additional air into the inlet. In this work, we computed mass capture increase with a virtual cowl at Mach numbers of 5 and 6. Figure 2 shows the contour lines of Mach number and streamlines in off-design Mach 6, $q = 1000$ psf (47.88 kPa) case, with no heat addition, when the air mass capture is only 0.815. In a series of virtual cowl computations, the heating profile was assumed to be elliptical Gaussian with the effective radii $r_{x,\mathrm{eff}} = 0.75$ m and $r_{z,\mathrm{eff}} = 0.1$ m, and the heated region was centered at its optimum location: near the intersection of the nose shock with the cowl line and slightly below that line, $Z_q = -1$ m, $x_q = 10.5$ m, as illustrated in Fig. 3.

Several computations were run with this location and shape of the heated region, with power input from 2.5 to 10 MW/m, that is, from 0.74 to 2.7% of the total enthalpy flux through the inlet. The resulting mass capture increases are correspondingly from 5.1 to 16.6%, and both compression ratios and kinetic energy efficiencies (reflecting the stagnation pressure) also increase (see Table 2 and Fig. 4).

Generally, plasmas can be generated near surfaces with higher overall efficiency and more control than far from the surfaces, in the free space. Therefore, it would be useful to assess the performance of a virtual cowl located close to the cowl surface where energy delivery can be more efficient. We have run a case with the same elliptical Gaussian heat-addition profile as the optimally located virtual cowl, but inclined at $\varphi = -4$ deg with respect to the x axis and located closer to the cowl lip, with coordinates $z_q = -0.5$ m, $x_q = 18.5$ m, as shown in Fig. 5.

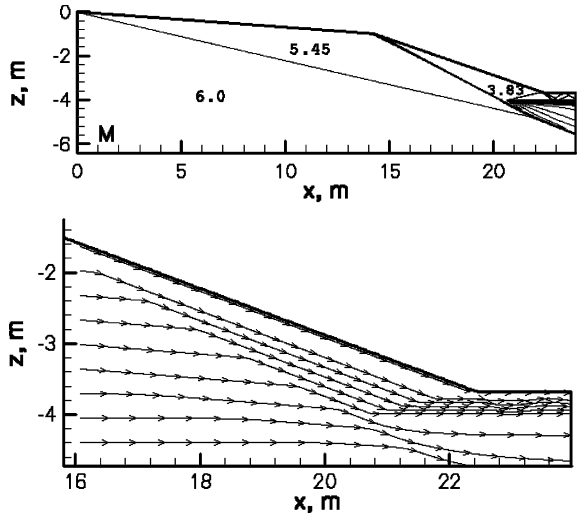

Fig. 2 Contour lines of Mach number and streamlines in off-design Mach 6, $q = 1000$ psf (47.88 kPa) case, with no heat addition.

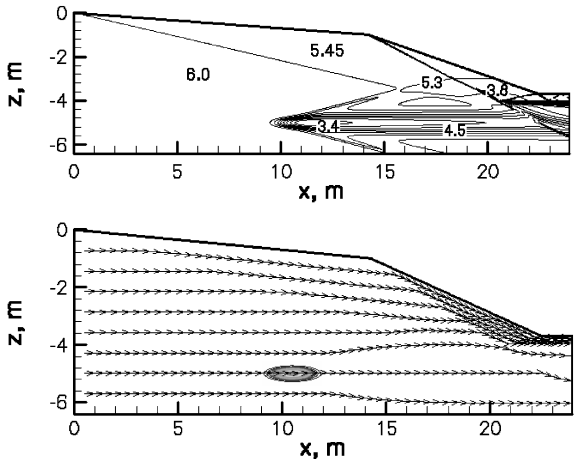

Fig. 3 Contour lines of static temperature, Mach number, and flow streamlines in off-design Mach 6, $q = 1000$ psf (47.88 kPa) case, with virtual cowl, at 10-MW/m heat-addition rate.

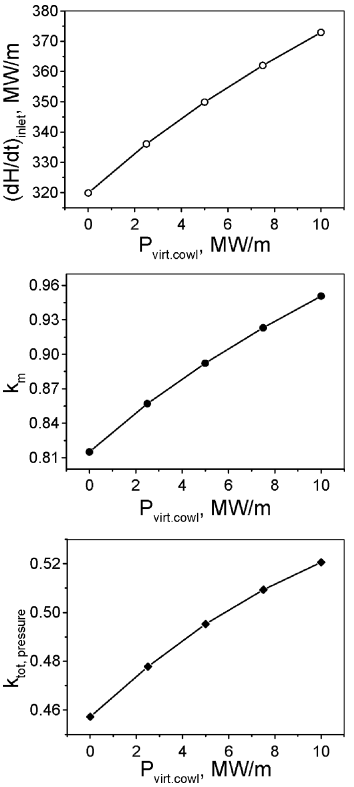

Fig. 4 Performance of the optimally located virtual cowl at off-design Mach 6: total enthalpy flux and thrust-averaged mass capture and total pressure coefficients vs heat-addition rate.

At a heating rate of 10 MW/m = 2.84% of the total enthalpy flux, the increase in mass capture in this case turned out to be 9.9%, considerably less than the 16.6% in the optimally located virtual cowl case, but still quite significant for the tradeoff between performance and the efficiency of heat delivery to be meaningful.

Calculations similar to those at Mach 6 were also performed for the Mach 5 off-design case. Figure 6 illustrates the flowfield without a virtual cowl, with mass spillage, and Fig. 7 shows the Mach-number contours with an optimally located virtual cowl. The virtual cowl had an elliptical Gaussian profile with the effective radii $r_{x,\mathrm{eff}} = 0.95$ m, $r_{z,\mathrm{eff}} = 0.1$ m; the profile was inclined at $\varphi = -4$ deg with respect to the negative direction of x axis and was centered at $z_q = -0.5$ m, $x_q = 14$ m (optimum location).

The results listed in Table 2 indicate that with the heat-addition rate between 2.5 and 8 MW/m, that is, between about 1 and 3% of the

Table 2 Computed cases and principal performance parameters for inlet/isolator control with energy addition: mass capture k_m, compression ratio k_p, adiabatic kinetic energy efficiency $\eta_{KE,ad}$, average Mach number at the throat $\langle M \rangle$, enthalpy capture ratio k_H, and the enthalpy flux through the throat $\dot{H}$

Flight Mach number, dynamic pressure, and energy addition rate (power)	k_m	k_p	$\eta_{KE,ad}$	$\langle M \rangle$	k_H	$\dot{H}$, MW/m
$M = 7$, $q = 1000$ psf (47.88 kPa), power = 0 (design)	0.957	61.4	0.970	2.81	1	425.9
$M = 4$, power = 0	0.55	45.89	0.958	1.1	1	180.75
$M = 5$, power = 0	0.679	43.71	0.958	1.85	1	232.4
Inlet Mach-number reduction by heat addition upstream of the throat						
$M = 5$, power $= 10.5 + (0.75 \times 4.5)_{cowl} + (0.25 \times 4.5)_{ramp}$ $= 15$ MW/m $= 6.3\%\ \dot{H}$	0.65	67.56	0.914	1.3	1.07	236.3
$M = 5$, power $= 13 + (0.75 \times 7)_{cowl} + (0.25 \times 7)_{ramp} = 20$ MW/m $= 8.5\%\ \dot{H}$	0.63	78.79	0.9023	1.15	1.092	234.4
Virtual cowl: $r_{x,eff} = 0.95$ m, $r_{z,eff} = 0.1$ m; $\varphi = -4^0$, $z_q = -0.5$ m, $x_q = 14$ m						
$M = 5$, power $= 2.5$ MW/m $= 1.03\%\ \dot{H}$	0.7 (+3%)	44.37	0.961	1.87	1	240.7
$M = 5$, power $= 5$ MW/m $= 2.014\%\ \dot{H}$	0.724 (+6.6%)	45.84	0.963	1.87	1	248.2
$M = 5$, power $= 8$ MW/m $= 3.12\%\ \dot{H}$	0.748 (+10.1%)	49.9	0.962	1.80	1	256.1
$M = 6$, power = 0	0.815	50.79	0.965	2.38	1	319.9
Virtual cowl: $r_{x,eff} = 0.75$ m, $r_{z,eff} = 0.1$ m; $\varphi = 0$, $z_q = -1$ m, $x_q = 10.5$ m						
$M = 6$, power $= 2.5$ MW/m $= 0.743\%\ \dot{H}$	0.857 (+5.1%)	53.58	0.967	2.37	1	336.17
$M = 6$, power $= 5$ MW/m $= 1.428\%\ \dot{H}$	0.892 (+9.4%)	55.95	0.969	2.37	1	349.9
$M = 6$, power $= 7.5$ MW/m $= 2.07\%\ \dot{H}$	0.923 (+13.25%)	58.13	0.970	2.36	1	362.09
$M = 6$, power $= 10$ MW/m $= 2.68\%\ \dot{H}$	0.95 (+16.56%)	60.19	0.971	2.35	1	372.9
Virtual cowl close to the cowl lip: $r_{x,eff} = 0.75$ m, $r_{z,eff} = 0.1$ m; $\varphi = -4^0$, $z_q = -0.5$ m, $x_q = 18.5$ m						
$M = 6$, power $= 10$ MW/m $= 2.84\%\ \dot{H}$	0.896 (+9.9%)	57.27	0.968	2.34	1	351.59

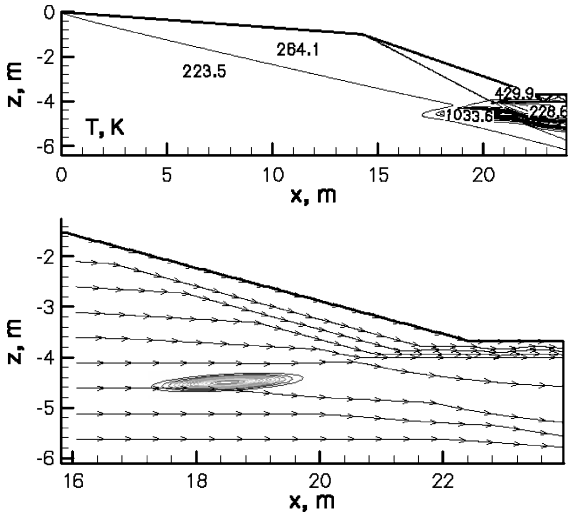

Fig. 5 Contour lines of static temperature and flow lines in off-design Mach 6, $q = 1000$ psf (47.88 kPa) case, with virtual cowl close to the cowl lip, at 10-MW/m heat-addition rate.

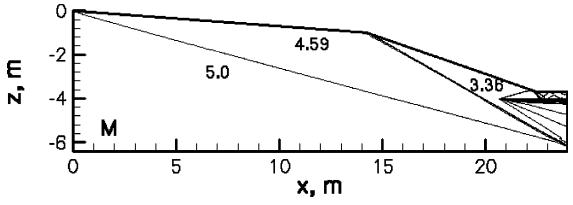

Fig. 6 Contour lines of Mach number in off-design Mach 5, $q = 1000$ psf (47.88 kPa) case, with no heat addition.

total inlet enthalpy flux, the mass capture increases by 3–10%, with a slight increase in compression ratio and kinetic energy efficiency.

As seen in Table 2, virtual cowl actually increases not only the mass capture, but also the kinetic energy efficiency; the latter reflects the increase in the stream-thrust-averaged total pressure at the throat. The reason for this is that the virtual cowl is deliberately placed slightly below the cowl line, so that the heated air misses the inlet, and only relatively "fresh," cold air is scooped (see also Ref. 14).

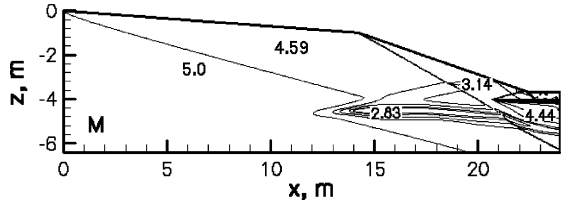

Fig. 7 Contour lines of Mach number in off-design Mach 5, $q = 1000$ psf (47.88 kPa) case, with virtual cowl at 8-MW/m heat-addition rate.

As seen in Figs. 3 and 5, the virtual cowl does generate shocks. However, these shocks are weak and do not have a significant effect on the stream-thrust-averaged inlet parameters.

B. Shortening the Isolator by Heat Addition Upstream of the Inlet Throat

In this section, we theoretically explore a possibility of minimizing the need for the traditional isolator stage using active control based on energy addition upstream of the inlet throat.[3] The energy addition can be accomplished by, for example, microwave plasma heating, electron beams, or localized plasma-assisted combustion.

Inlet geometry is that in Fig. 1, and the stream-thrust-averaged Mach number at the throat in the off-design Mach 5 case with no heat addition (Fig. 6) is 1.85, so that an isolator duct would normally be required to reduce the Mach number (as well as to mix the flow properly).

We then placed three distributed heating sources upstream of the throat, as shown in the upper plot of Fig. 8. The total heating rate was 15 MW/m (6.3% of the enthalpy flux through the throat), consisting of 10.5 MW/m between the cowl and the compression ramp, 3.375 MW/m at the cowl, and 1.125 MW/m at the ramp. The resulting flowfield is shown in Fig. 8, and the principal inlet performance parameters are listed in Table 2. The stream-thrust-averaged Mach number at the throat is now 1.3.

Increasing the heating rate further reduces the throat Mach number, as shown in Fig. 9, where the total heating rate is 20 MW/m (8.5% of the enthalpy flux through the throat), consisting of 13 MW/m between the cowl and the compression ramp, 5.25 MW/m at the cowl, and 1.75 MW/m at the ramp. The stream-thrust-averaged Mach number at the throat is now 1.15 (see Table 2), and the isolator duct can perhaps be eliminated.

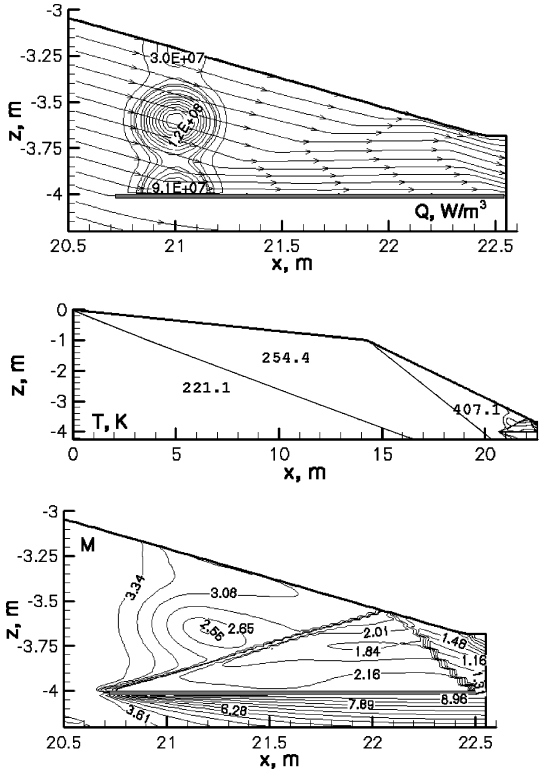

Fig. 8 Power deposition density and contour lines of static temperature and Mach number in Mach 5, 1000 psf (47.88 kPa) off-design case. Total heating rate is 15 MW/m (6.3% of the enthalpy flux through the throat), consisting of 10.5 MW/m between the cowl and the compression ramp, 3.375 MW/m at the cowl, and 1.125 MW/m at the ramp.

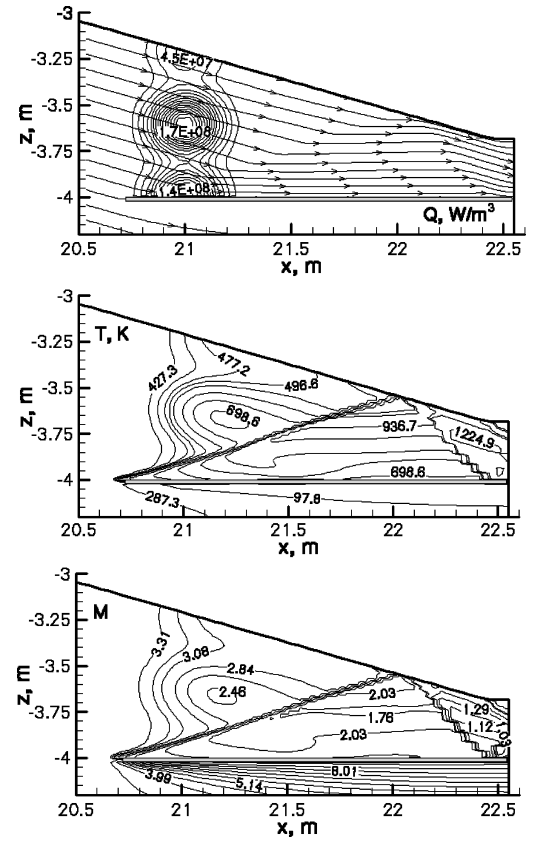

Fig. 9 Power deposition density and contour lines of static temperature and Mach number in Mach 5, 1000 psf (47.88 kPa) off-design case. Total heating rate is 20 MW/m (8.5% of the enthalpy flux through the throat), consisting of 13 MW/m between the cowl and the compression ramp, 5.25 MW/m at the cowl, and 1.75 MW/m at the ramp.

These calculations demonstrate that, in principle, heating the flow upstream of the inlet throat can condition the flow in such a way that an isolator duct would be unnecessary. Implementation of this approach depends on whether the required amount of power can be generated and delivered at these relatively low flight Mach numbers, and whether the stagnation pressure losses in dissipative processes in the heated region and in the downstream MHD generator would still leave sufficient thrust to accelerate the vehicle.

III. MHD Generator Downstream of Combustor as a Power Source for Virtual-Shape Inlet Control: Assessment of Performance of Reverse Energy Bypass Concept

One way of supplying the energy for the virtual cowl (Sec. II.A) or inlet heating (Sec. II.B) would be to extract energy from the flow with an MHD generator placed downstream of the combustor and to then deliver this energy to the desired location upstream of the inlet throat using dc, rf, or microwave plasma sources. In an evaluation of the performance of this reverse energy bypass concept, losses of energy and stagnation pressure in all of the system components must be taken into account.

In this work, we adopted a linearized approach whereby percent changes of the thrust are calculated for each system component independently, and the results are summed algebraically. This approach is obviously justified if the percent changes of the thrust are relatively small.

Parameters of the MHD generator placed downstream of the combustor were calculated for conditions corresponding to Mach 5 and Mach 6 flight at $q = 1000$ psf (47.88 kPa) with the one-dimensional model of Ref. 3. Combustor exit and MHD inlet conditions at Mach 5 and Mach 6 (Tables 3–5) were those listed in Ref. 3 for a typical hydrogen-fueled ram/scramjet at an equivalence ratio of 1. The geometric parameters of the MHD generator (inlet height z_{in} and exit height z_L) are listed in Tables 3, 4, and 6. Potassium seed fraction in all cases was $\eta_K = 1\%$, and the load factor was either $k = 0.5$ or 0.9. The strength of the magnetic field was varied between 1.5 and 3.4 T. The results are summarized in Tables 3–5. Note that in modeling the MHD generator, as well as subsequent flow expansion, enthalpy and entropy definitions were those used in chemical thermodynamics, including enthalpies of formation of mixture constituents. Therefore, the enthalpy extraction ratio values listed in Tables 3–5 are different from values that would have been calculated if combustion were modeled as heat addition to a gas with constant composition.

As seen in Tables 3–5, an MHD generator with reasonable length (1 m), seed fraction (1%), and 1.5–3.4 T magnetic fields can indeed produce more than enough power to heat the flow upstream of the inlet and eliminate the need for an isolator duct (at least 20 MW/m) and to operate a virtual cowl for mass capture increase (at least 10 MW/m).

In the thrust computations, friction and heat losses were neglected, and the flow from the combustor or MHD generator exit to the final exit plane (the vertical projection from the vehicle tail to the cowl line) was assumed one dimensional, isentropic, and thermochemically equilibrium. Thus, the conditions at the final exit plane (index 2) are related to the conditions at the combustor or MHD generator exit (index 1) with the set of equations:

$$\rho_1 u_1 a_1 = \rho_2 u_2 a_2, \qquad u_1^2/2 + h_1 = u_2^2/2 + h_2$$

$$s_1 = s_2, \qquad P_2 = [(\gamma - 1)/\gamma]\rho_2 h_2 \tag{1}$$

where ρ is the density, p is the pressure, u is the velocity, h is the specific static enthalpy, s is the specific entropy, γ is the specific heat ratio, and a is the cross-section area per unit length in the spanwise direction. The areas a in Eqs. (1) were taken as $a_1 = z_{\text{in}}$ in the case with no MHD, $a_2 = z_L$, in MHD cases, and $a_2 = \Delta z_{\text{out}} = 8$ m. Thus, the overall area ratio $\Delta z_{\text{out}}/\Delta z_{\text{in}}$ between the final exit plane and the inlet capture plane was equal to 2.

Because the parameters at the final exit plane varied within limited ranges, the approximation of an ideal gas with constant specific

Table 3 Parameters of the MHD generator (magnetic field B, generated power P_{MHD}, and enthalpy extraction ratio η) and MHD exit conditions (p, T, u, and M)[a]

Case	B, T	z_l/z_{in}	k	P_{MHD}, MW/m	η, %	p, Pa after MHD	T, K after MHD	u, m/s after MHD	M after MHD
1.1	1.5	1.5	0.5	21.0	9.26	78,219.7	2,388.7	1,385.7	1.42
1.2	2.5225	1.5	0.9	21.0	9.26	68,396.1	2,318.1	1,528.5	1.59
1.3	2.0	1.75	0.5	38.7	17.07	78,666.1	2,426.5	1,204.7	1.22
1.4	3.38225	1.75	0.9	38.7	17.07	61,694.8	2,299.6	1,458.2	1.48

[a]Inlet geometry is designed for Mach 7; the actual flight Mach number is 5 at $q = 1000$ psf (47.88 kPa). Combustor exit and MHD inlet conditions are $u(0) = 1291$ m/s, $T(0) = 2519$ K, and $p(0) = 1.327$ atm (0.1344 MPa). Potassium seed fraction is $\eta_K = 1\%$. Inlet mass capture coefficient is $k_m = 0.65$. The load factor is $k = 0.5$ or 0.9. Geometric parameters of the MHD generator are $L = 1$ m; $z_{in} = 0.85$.

Table 4 Same as in Table 3, except that the inlet mass capture coefficient is $k_m = 0.85$, and the height of the MHD generator inlet is $z_{in} = 1.11$ m

Case	B, T	z_l/z_{in}	k	P_{MHD}, MW/m	η, %	p, Pa after MHD	T, K after MHD	u, m/s after MHD	M after MHD
1.5	1.5	1.5	0.5	27.27	9.26	78,219.7	2,388.7	1,385.7	1.42
1.6	2.5225	1.5	0.9	27.2	9.26	68,396.1	2,318.1	1,528.5	1.59

Table 5 Parameters of the MHD generator (magnetic field B, generated power P_{MHD}, and enthalpy extraction ratio η) and MHD exit conditions (p, T, u, and M)[a]

Case	B, T	k_m	k	P_{MHD}, MW/m	η, %	p, Pa after MHD	T, K after MHD	u, m/s after MHD	M after MHD
2.1	1.5	0.95	0.5	39.36	10.22	83,454.4	2,495.1	1,480.6	1.48
2.2	2.522	0.95	0.9	39.36	10.22	70,371.3	2,392.4	1,673.6	1.72
2.3	1.5	0.896	0.5	37.29	10.22	83,454.4	2,495.1	1,480.6	1.48
2.4	2.522	0.896	0.9	37.28	10.22	70,371.1	2,392.4	1,673.6	1.73
2.5	1.0	0.896	0.5	16.87	4.6	70,001.0	2,411.1	1,699.3	1.73
2.6	1.6875	0.896	0.9	16.86	4.6	65,312.5	2,366.7	1,778.1	1.83

[a]Inlet geometry is designed for Mach 7; the actual flight Mach number is 6 at $q = 1000$ psf (47.88 kPa). Combustor exit and MHD inlet conditions are $u(0) = 1574.5$ m/s, $T(0) = 2590.9$ K, and $p(0) = 1.184$ atm. Geometric parameters of the MHD generator are $L = 1$ m; $z_{in} = 0.95$ m at $k_m = 0.95$ ($P_{VCL} = 10$ MW/m with the optimum location of virtual cowl), and $z_{in} = 0.9$ m at $k_m = 0.896$ ($P_{VCL} = 10$ MW/m with the virtual cowl close to the cowl lip); in all cases $z_L/z_{in} = 1.5$. Potassium seed fraction is $\eta_K = 1\%$.

Table 6 Thrust component values for the cases of inlet heating for throat Mach number reduction[a]

Case	k_m	F_1, N/m	F_2^0, N/m (no MHD)	F_2, N/m (with MHD)	$(F_2 - F_2^0)/F_2^0$, %	$[\Delta(F_2 - F_1)/(F_2^0 - F_1)]_{MHD}$, %	$\Delta(F_2 - F_1)/(F_2^0 - F_1^0)$, %
1.1	0.65	255,504.7	457,942.7	435,375.4	−4.9	−11.1	−16
1.2	0.65	255,504.7	457,942.7	440,380.8	−3.8	−8.6	−14
1.3	0.65	255,504.7	457,942.7	425,162.1	−7.2	−16.2	−21
1.4	0.65	255,504.7	457,942.7	434,896.0	−5.0	−11.4	−16
1.5	0.85	334,121.6	586,411.2	550,995.1	−6.0	−14.0	−19
1.6	0.85	334,121.6	586,411.2	558,165.6	−4.8	−11.2	−16

[a]All case are for Mach 5, $q = 1000$ psf (47.88 kPa) flight with the inlet designed for Mach 7 shock-on-lip. The front-end force is $F_1 = k_m(\rho_0 u_0^2 + p_0)\Delta z(0)$ with $\Delta z(0) = 4$ m. The force acting at the exit cross section $F_2 = (\rho_{out} u_{out}^2 + p_{out})\Delta z_{out}$ corresponds to isentropic expansion from MHD generator (or combustor, in the case without MHD) to the exit with $\Delta z_{out} = 8$ m. The total relative thrust change $\Delta(F_2 - F_1)/(F_2^0 - F_1)$ values are shown in the last column.

heats was used for the equation of state at station 2. To find the necessary parameters for this equation of state, including the specific heats and the reference enthalpy and entropy, the ideal-gas formulas were calibrated against ASTRA commercial software for calculations of thermochemical equilibrium.[15] The calibration yielded the following parameters for the exit equilibrium stoichiometric hydrogen-air mixture: $\gamma = 1.3$, $c_p = 1442$ J/kg, $h = c_p T - 3.75 \cdot 10^6$ J/kg, and $s = c_v \ln(p/p^\gamma) - 5051.18$ J/kg.

With the fully specified flowfield, the sums of the pressure force and the momentum flux at the inlet capture plane, $F_1 = k_m(\rho_0 u_0^2 + p_0)\Delta z(0)$ with $\Delta z(0) = 4$ m (k_m is the inlet mass capture coefficient), and at the final exit plane, $F_2 = (\rho_{out} u_{out}^2 + p_{out})\Delta z_{out}$, were computed. The net thrust was then found as $F_2 - F_1$. For example, in the design regime at Mach 7, $q = 1000$ psf (47.88 kPa), $F_1 = 378656.7$ N/m, $F_2 = 528375.8$ N/m, and $F_2 - F_1 = 149719.1$ N/m. Tables 6–8 list the computed thrust components F_1 and F_2, the force acting at the final exit cross section in the baseline case with no MHD and no inlet control F_2^0, the percent change in F_2 with respect to the baseline cases $(F_2 - F_2^0)/F_2^0$, and the relative thrust change $\Delta(F_2 - F_1)/(F_2^0 - F_1)$ values.

To evaluate thrust changes caused by the inlet heating, the values of mass capture coefficient k_m, enthalpy capture coefficient k_H, and kinetic energy efficiency $\eta_{KE.ad}$ listed in Table 2 were used together with the sensitivities of the thrust with respect to these parameters provided by D. Van Wie of Johns Hopkins University Applied Physics Laboratory. The resulting change in thrust caused by the 20-MW/m inlet heating was estimated to be about −5%. This is reflected in Table 6, where the total percent thrust changes (last column) were calculated by subtracting 5 from the values in the second column from the right.

The overall performance of the energy bypass system with inlet heating depends on the efficiency of transmission of the MHD-generated power to the inlet heating plasma. Because the inlet heating occurs in a duct, a dc or rf plasma can be run with direct

Table 7 Effect of MHD generator on thrust in $M = 6$, $q = 1000$ psf (47.88 kPa) case with mass capture $k_m = 0.815$ (no virtual cowl)[a]

Case	k	B, T	η, %	F_2, N/m (with MHD)	$(F_2 - F_2^0)/F_2^0$, %	$[\Delta(F_2 - F_1)/(F_2^0 - F_1^0)]_{\text{MHD}}$, %
2.1, 2.3	0.5	1.5	10.22	493,278.6	−4.6	−11.6
2.2, 2.4	0.9	2.5225	10.22	502,462.3	−2.8	−7.2
2.5	0.5	1.0	4.6	507,469.4	−1.9	−4.7
2.6	0.9	1.6875	4.6	510,198.4	−1.3	−3.4

[a]The front-end force is $F_1 = k_m(\rho_0 u_0^2 + p_0)\Delta z(0)$ with $\Delta z(0) = 4$ m. The force acting at the exit cross section $F_2 = (\rho_{\text{out}} u_{\text{out}}^2 + p_{\text{out}})\Delta z_{\text{out}}$ corresponds to isentropic expansion from MHD generator (or combustor, in the case without MHD) to the exit with $\Delta z_{\text{out}} = 8$ m. The baseline (no MHD) parameters are: $F_1 = 382688.7\ k_m = 311891.3$ N/m, $F_2^0 = 517265.4$ N/m, and $F_2^0 - F_1 = 134576.7$ N/m. k is the load factor, η is the enthalpy extraction ratio, B is the magnetic field induction. The geometric parameters of MHD generator are: $L = 1$ m, $z_{\text{in}} = 0.85$, and $z_L/z_{\text{in}} = 1.5$.

Table 8 Total thrust change $\Delta(F_2 - F_1)/(F_2^0 - F_1^0) \approx \Delta k_m/k_{m0} + [\Delta(F_2 - F_1)/(F_2^0 - F_1^0)]_{\text{MHD}}$, for the cases with virtual cowl listed in Table 5

Case	$\Delta k_m/k_{m0}$, %[a]	$[\Delta(F_2 - F_1)/(F_2^0 - F_1^0)]_{\text{MHD}}$, %	$\Delta(F_2 - F_1)/(F_2^0 - F_1^0)$, %
2.1	+16.6	−11.6	+5.0
2.2	+16.6	−7.2	+9.4
2.3	+9.9	−11.6	−1.7
2.4	+9.9	−7.2	+2.7
2.5	+9.9	−4.7	+5.7
2.6	+9.9	−3.4	+6.5

[a]k_{m0} corresponds to the baseline case with no virtual cowl.

connection to the MHD generator, so that nearly all generated power can be deposited in the inlet. This corresponds to cases 1.1 and 1.2 of Tables 3 and 6. To minimize stagnation pressure losses in the MHD generator because of dissipative Joule heating, the load factor should be close to 1, and to maintain the extracted power the magnetic field should be increased. Indeed, case 1.2 has $k = 0.9$ and $B = 2.5$ T and yields somewhat lower thrust reduction (−14%) than case 1.2 with $k = 0.5$ and $B = 1.5$ T does (−16%).

Cases 1.3–1.6 correspond to situations with substantial losses in conditioning and transmission of the generated power to the inlet plasma. For example, cases 1.5 and 1.6 assume 73.5% efficiency of power conditioning and transmission, and cases 1.3 and 1.4 assume 52% efficiency. In these cases, however, despite the substantial power losses the thrust reduction can be maintained at the level of −16% with the load factor $k = 0.9$ and the appropriate magnetic field (Tables 3, 4, and 6). The 16% reduction in thrust can leave enough thrust to accelerate the vehicle, while eliminating the isolator duct and thus increasing performance at cruise.

In assessing the performance of the reverse bypass system with an MHD generator powering a virtual cowl, the results of evaluation of the virtual cowl effect on thrust performed by D. Van Wie of Johns Hopkins University Applied Physics Laboratory[3] were used. Specifically, as shown in Ref. 3, the increase in thrust is nearly equal to the increase in mass capture coefficient because of the virtual cowl. This is reflected in Table 8, where the total thrust change for the reverse bypass system with virtual cowl is the algebraic sum of the thrust changes caused by the mass capture increase and those caused by the MHD generator (the latter values were taken from Table 7).

In the case of a virtual cowl in its optimum location, far from the vehicle surface (Fig. 3) the required energy would have to be deposited by, for example, a freely localized plasma created by a phased microwave array. In this case, the efficiency of energy transmission from the MHD generator to the freely localized microwave plasma would be quite low, perhaps as low as 25%: for a heating rate of 10 MW/m, about 40 MW/m would have to be generated. Cases 2.1 and 2.2 in Tables 5, 7, and 8 correspond to this low efficiency of power transmission. With the virtual cowl located close to the cowl lip (Fig. 5), the power can be again transmitted by a microwave array with 25% efficiency (cases 2.3 and 2.4), but because of the proximity of the surfaces dc or rf discharges could conceivably also be run. In the latter case, 54% power transmission efficiency was assumed (cases 2.5 and 2.6).

As seen in Tables 7 and 8, the MHD generation of power required for the virtual cowl leads to a substantial reduction in thrust, both because of the need to generate enough power to compensate for conditioning and transmission losses and because of the dissipative Joule heating. The latter, as seen from a comparison of cases 2.1, 2.3, and 2.5 with cases 2.2, 2.4, and 2.6, respectively, can be minimized by operating with a load factor close to 1 and the appropriate increase in magnetic field strength to maintain the required power level.

The best performance for the reverse energy bypass with an optimally located virtual cowl (case 2.2) is a 9.4% thrust increase, while thrust increase with the virtual cowl close to the cowl lip (case 2.6) is 6.5%. The choice between the two scenarios would involve trading performance for practicality.

IV. Conclusions

In this paper, we explored the concept of ram/scramjet propulsion control by energy addition and extraction in the propulsion flowpath. Instead of variable geometry, the concept relies on virtual shapes created by plasma/MHD devices. An inherent advantage of the proposed plasma/MHD control system is its flexibility, fast response, and the absence of moving parts.

The fixed geometry was optimized for Mach 7 flight. At Mach numbers below the design value, inlet performance can be improved by energy addition, with the power supplied by an MHD generator placed downstream of the combustor. This concept has been called the reverse energy bypass in this paper. In the reverse bypass concept, MHD generation of power required for inlet control leads to substantial reduction in system performance, both because of the need to generate enough power to compensate for conditioning and transmission losses and because of the dissipative Joule heating. The latter, as shown in the paper, can be minimized by operating with a load factor close to 1 and the appropriate increase in magnetic field strength to maintain the required power level.

In one reverse bypass scenario, the inlet flow spillage can be reduced by a virtual cowl—a heated region placed upstream of the cowl and slightly below it. With an optimally located virtual cowl, calculations with conservative assumptions regarding power transmission efficiency (as low as 25%) show that the reverse bypass can increase thrust by about 10% at Mach 6.

In another scenario, distributed heating of the flow upstream of the inlet throat in the ramjet regime (Mach 4–6), with the heating rate of about 6.3–8.5% of the total enthalpy flux, can bring

the throat Mach number close to 1, thus making the isolator duct virtually unnecessary. In this reverse bypass system, total pressure losses caused by the inlet heating and the losses caused by the MHD power generation and ransmission would result in thrust reduction by about 16% at Mach 5. Whether the performance penalty at the vehicle acceleration stage can be offset by the increased efficiency during the cruise because of the absence of weight and cooling burden normally caused by the long isolator duct should be determined by a detailed system analysis for a specific mission. The additional weight and complexity associated with both MHD power generator and the plasma heating should also be incorporated into such analysis.

Being the first, preliminary, assessment of potential performance of the reverse energy bypass concept, the analysis in this paper was, naturally, simplified, combining two-dimensional inviscid computations of the inlet flow with heat addition with quasi-one-dimensional flowpath calculations downstream of the inlet. Full evaluation of the proposed concept should include three-dimensional time-dependent viscous flow dynamics, vibrational excitation and relaxation, fuel-air mixing, and finite-rate combustion chemistry. However, the performance predictions made in this paper, especially given the very conservative assumptions regarding the power transmission losses, are encouraging enough to warrant further studies with more sophisticated models.

Acknowledgments

This work was supported by Boeing Phantom Works, DARPA, and by the Air Force Office of Scientific Research. The authors express their gratitude to Richard Miles of Princeton University and to Joseph Silkey of Boeing Phantom Works for advice and numerous discussions. We are deeply grateful to David Van Wie of Johns Hopkins University Applied Physics Laboratory for sharing his knowledge and experience and providing invaluable advice and patient guidance.

References

[1]Curran, E. T., and Murthy, S. N. B., (eds.), *Scramjet Propulsion*, Progress in Astronautics and Aeronautics, Vol. 189, AIAA, Reston, VA, 2000.

[2]Van Wie, D. M., "Scramjet Inlets," *Scramjet Propulsion*, edited by E. T. Curran and S. N. B. Murthy, Progress in Astronautics and Aeronautics, Vol. 189, AIAA, Reston, VA, 2000, Chap. 7, pp. 447–511.

[3]Shneider, M. N., Macheret, S. O., Miles, R. B., and Van Wie, D. M., "MHD Power Generation in Scramjet Engines in Conjunction with Inlet Control," AIAA Paper 2004-1197, Jan. 2004.

[4]Macheret, S. O., Shneider, M. N., and Miles, R. B., "Optimum Performance of Electron Beam Driven MHD Generators for Scramjet Inlet Control," AIAA Paper 2003-3763, June 2003.

[5]Shneider, M. N., Macheret, S. O., and Miles, R. B., "Analysis of Magnetohydrodynamic Control of Scramjet Inlets," *AIAA Journal*, Vol. 42, No. 11, 2004, pp. 2303–2310.

[6]Shneider, M. N., Macheret, S. O., and Miles, R. B., "Comparative Analysis of MHD and Plasma Methods of Scramjet Inlet Control," AIAA Paper 2003-170, Jan. 2003.

[7]Kuranov, A. L., and Sheikin, E. G., "MHD Control on Hypersonic Aircraft under AJAX Concept: Possibilities of MHD Generator," AIAA Paper 2002-0490, Jan. 2002.

[8]Macheret, S. O., Shneider, M. N., and Miles, R. B., "External Supersonic Flow and Scramjet Inlet Control by MHD with Electron Beam Ionization," AIAA Paper 2001-492, Jan. 2001.

[9]Macheret, S. O., Shneider, M. N., and Miles, R. B., "Magnetohydrodynamic Control of Hypersonic Flow and Scramjet Inlets Using Electron Beam Ionization," *AIAA Journal*, Vol. 40, No. 1, 2002, pp. 74–81.

[10]Macheret, S. O., Shneider, M. N., and Miles, R. B.,"Magnetohydrodynamic and Electrohydrodynamic Control of Hypersonic Flows of Weakly Ionized Plasmas," *AIAA Journal*, Vol. 42, No. 7, 2004, pp. 1378–1387.

[11]Macheret, S. O., Shneider, M. N., Miles, R. B., Lipinski, R. J., and Nelson, G. L., "MHD Acceleration of Supersonic Air Flows Using Electron Beam-Enhanced Conductivity," AIAA Paper 1998-2922, June 1998.

[12]Macheret, S. O., Shneider, M. N., and Miles, R. B., "MHD Power Extraction from Cold Hypersonic Air Flow with External Ionizers," *Journal of Propulsion and Power*, Vol. 18, No. 2, 2002, pp. 424–431.

[13]Macheret, S. O., Shneider, M. N., Miles, R. B., and Lipinski, R. J., "Electron Beam Generated Plasmas in Hypersonic Magnetohydrodynamic Channels," *AIAA Journal*, Vol. 39, No. 6, 2001, pp. 1127–1136.

[14]Macheret, S. O., Shneider, M. N., and Miles, R. B., "Scramjet Inlet Control by Off-Body Energy Addition: a Virtual Cowl," *AIAA Journal*, Vol. 42, No. 11, 2004, pp. 2294–2302.

[15]Trusov, B. G., "ASTRA," Computer Program for Calculation of Thermodynamic Properties of Individual Substances and Mixtures, Moscow Bauman Technical Univ., Moscow, 2001.